RKIP suppresses the influenza A virus-induced airway inflammatory response via the ERK/MAPK pathway

JING-JING YE[1,2*], SI-LIANG WEI[1,2*], YUAN-YUAN WEI[1,2], DA-WEI ZHANG[1,2], LI SUN[1,2], HUI-MEI WU[3], JI-LONG SHEN[4], LI YU[4], YONG WANG[1,2] and GUANG-HE FEI[1,2]

[1]Department of Respiratory and Critical Care Medicine, [2]Key Laboratory of Respiratory Diseases Research and Medical Transformation of Anhui Province, First Affiliated Hospital of Anhui Medical University; [3]Department of Geriatric Respiratory and Critical Care, Anhui Geriatric Institute, First Affiliated Hospital of Anhui Medical University; [4]Department of Pathogen Biology and Provincial Laboratories of Pathogen Biology and Zoonoses, Anhui Medical University, Hefei, Anhui 230022, P.R. China

Received August 2, 2022; Accepted October 24, 2022

DOI: 10.3892/ijmm.2022.5204

Abstract. Raf kinase inhibitor protein (RKIP) is an inflammation-inhibiting mediator that is involved in several diseases; however, the potential mechanism of action of RKIP on the inflammatory response induced by influenza A virus (IAV) remains unclear. The present study aimed to investigate whether RKIP regulated the inflammatory response via the ERK/MAPK pathway. The present study detected the expression levels of RKIP and alterations in the inflammatory response in human normal bronchial epithelial BEAS-2B cells, diseased human bronchial epithelial cells and primary human bronchial epithelial cells infected with IAV. Cells were treated with locostatin to inhibit the expression of RKIP. RKIP was overexpressed by lentivirus transduction and the small molecule inhibitor SCH772984 was applied to specifically inhibit activation of the ERK/MAPK pathway. In addition, C57BL/6 mice were infected with IAV to further confirm the role of RKIP in regulation of the inflammatory response via ERK/MAPK *in vivo*. Western blotting, reverse transcription-quantitative PCR, ELISA, 5-ethynyl-2'-deoxyuridine assay, immunofluorescence staining, Cell Counting Kit-8, cell cycle assay, hematoxylin and eosin staining, and immunohistochemistry were used to detect all of the changes. Notably, RKIP attenuated the inflammatory response that was triggered by IAV infection in airway epithelial cells, which was characterized by augmented inflammatory cytokines and cell cycle arrest. Furthermore, the ERK/MAPK pathway was revealed to be activated by IAV infection and downregulation of RKIP aggravated the airway inflammatory response. By contrast, overexpression of RKIP effectively ameliorated the airway inflammatory response induced by IAV. These findings demonstrated that RKIP may serve a protective role in airway epithelial cells by combating inflammation via the ERK/MAPK pathway. Collectively, the present findings suggested that RKIP may negatively regulate airway inflammation and thus may constitute a promising therapeutic strategy for airway inflammatory-related diseases that are induced by IAV.

Correspondence to: Professor Guang-He Fei or Professor Yong Wang, Department of Respiratory and Critical Care Medicine, First Affiliated Hospital of Anhui Medical University, 210 Jixi Road, Hefei, Anhui 230022, P.R. China
E-mail: gh.fei@ahmu.edu.cn
E-mail: wayt@sina.com

*Contributed equally

Abbreviations: AECOPD, acute exacerbation of chronic obstructive pulmonary disease; BALF, bronchoalveolar lavage fluid; CCK-8, Cell Counting Kit-8; DHBE, diseased human bronchial epithelial; EdU, 5-ethynyl-2'-deoxyuridine; H&E, hematoxylin and eosin; IAV, influenza A virus; MOI, multiplicity of infection; NLRP, NLR family pyrin domain-containing; PEBP, phosphatidylethanolamine-binding protein; pNHBE, primary human bronchial epithelial; RT-qPCR, reverse transcription-quantitative PCR; RKIP, Raf kinase inhibitor protein

Key words: IAV, RKIP, airway inflammation, cell cycle, ERK/MAPK

Introduction

Influenza A virus (IAV) is a principal pathogen of infectious respiratory diseases (1) and a common trigger for a number of other respiratory diseases, such as acute exacerbation of chronic obstructive pulmonary disease (AECOPD) (2). Severe IAV infection contributes significantly to substantial morbidity and mortality, and is responsible for health and economic burdens experienced worldwide (3,4). Numerous airway inflammatory responses are induced by respiratory viruses, leading to increased proinflammatory cytokines and the consequent development of cytokine storms (5). It is well known that the proinflammatory agents TNF-α and nitric oxide can interfere with cell cycle progression in different somatic cells, and it has been reported that TNF-α-generated oxidative stress can

reduce cellular proliferation and induce cell cycle arrest (6,7). Notably, the effect of TNF-α on L-cells is cytostatic, which manifests as cell cycle arrest in the G_2 stage, thus indicating that the cell cycle is dependent upon TNF cytotoxicity (8). While such data indicate that inflammation and the cell cycle may be linked, the molecular mechanisms that mediate IAV-induced airway inflammatory responses remain unclear.

Raf kinase inhibitor protein (RKIP) is a member of the phosphatidylethanolamine-binding protein (PEBP) family, and is a highly conserved small molecule protein that is primarily located in the cytoplasm and plasma membrane (9). By binding specifically to Raf-1 kinase, RKIP modulates crucial intracellular signaling networks that include the Raf/MEK/ERK, NF-κB and GSK-3β signaling cascades (1,3,l0-12). Several studies have revealed that RKIP participates in the regulation of a variety of physiological and pathological processes, such as cellular differentiation, cell cycle progression, apoptosis (11,13-15), autophagy, ferroptosis (16,17) and inflammation (18,19). The expression of RKIP has been reported to be enhanced by didymin, which results in inhibition of the MAPK and NF-κB pathways, and contributes to the anti-inflammatory effects of RKIP (20). It has been demonstrated that RKIP serves a negative role in regulating NLR family pyrin domain-containing (NLRP)1, NLRP3 and NLR family CARD domain-containing 4 inflammasome activation, and that it is a potential therapeutic target for the treatment of inflammasome-related diseases (21). It has also been reported that RKIP occupies a critical role in the cell cycle of numerous types of cancer (22). Although there are a considerable number of published reports linking RKIP to various intracellular signaling networks that control cellular growth (23-26), the effects exerted by RKIP on inflammation and cell cycle progression in airway epithelial cells following IAV infection have not yet been reported.

The present study investigated the detailed mechanisms underlying RKIP action in IAV-induced airway inflammation by adopting primary human bronchial epithelial (pNHBE) cells, cell lines and mouse models.

Materials and methods

Reagents and materials. Locostatin (cat. no. T8823) was purchased from Shanghai Topscience Co., Ltd. SCH772984 (cat. no. S7101) was purchased from Selleck Chemicals. RKIP (cat. no. ab76582) and β-actin (cat. no. ab8227) antibodies were purchased from Abcam. NLRP3 (cat. no. WL02635), ERK1/2 (cat. no. WL01864) and phosphorylated (p)-ERK1/2 (Thr202/Tyr204; cat. no. WLP1512) antibodies were purchased from Wanleibio Co., Ltd. CDK4 antibody (D9G3E; cat. no. 12790) was obtained from Cell Signaling Technology, Inc.

Animal experiments. C57BL/6 mice (female; age, 6 weeks; weight, 20-25 g; n=24) were purchased from the Animal Service Unit of Anhui Medical University. Mice were maintained at a controlled temperature (22-25˚C) and humidity (50-60%), under a 12-h light/dark cycle, and provided with free access to water and food. In the present study, mice were challenged with IAV to induce airway inflammation and treated with locostatin. Mice were randomly allocated to the following four groups (n=6/group): i) The negative control (NC) group: IAV(-) + locostatin(-); ii) IAV(+) + locostatin(-) group; iii) IAV(-) + locostatin(+) group; and iv) IAV(+) + locostatin(+) group. Locostatin (10 mg/kg) pretreatment was conducted for 4 h via intraperitoneal injection before 100 PFU of IAV was administered in 100 μl through oropharyngeal aspiration and the NC group was treated with 0.9% saline. After 7 days, mice were anesthetized with pentobarbital (70 mg/kg), and after euthanizing the mice, the serum, BALF and lung tissues were collected for further analysis. Blood was drawn by enucleation of the eyeball, followed by centrifugation at 3,000 x g for 5 min at 4˚C, and the serum was collected for subsequent experiments. To collect BALF, a needle was inserted into the trachea and fixed. The lungs were lavaged with 1 ml cold PBS three times to collect the BALF, followed by centrifugation at 500 x g for 10 min at 4˚C; the supernatants were collected for subsequent experiments. Mice health and behavior were monitored daily. During the experiment, any mice that were unable to drink or eat, had difficulty breathing or had lost 20% of their body weight were regarded as having reached the humane endpoints and were immediately euthanized. None of the mice reached the aforementioned endpoints in this experiment and thus none were euthanized before the end of the experiment. Every effort was made to minimize discomfort, distress, pain or injury to the mice. The total duration of the experiment was 7 days. After the experiment, all remaining animals were euthanized by cervical dislocation and death was verified by respiratory arrest, cardiac arrest and dilated pupils. All protocols were reviewed and approved by the Animal Ethics Committee of Anhui Medical University.

Cell isolation and culture. The pNHBE cells were isolated from the normal bronchial tissues of patients with lung carcinoma *in situ* (n=3; 2 women, 1 man; age, 48-52 years) as determined by senior pathologists. The bronchial tissues were cut at a site >3 cm distant from the edge of the lung carcinoma according to methods modified from previous studies (27-30) between August 2020 and January 2021, and were cultured in bronchial epithelial cell growth medium (Lonza Group, Ltd.). The present study was approved by the Biomedical Ethics Committee of Anhui Medical University (approval no. 20200070; Hefei, China). All of the participants were informed of the purpose of the study and provided written informed consent in accordance with the ethical requirements. Human airway epithelial BEAS-2B cells were purchased from Shanghai Fuheng Biotechnology Co., Ltd. (cat. no. FH0319) and cultured in RPMI-1640 medium (Hyclone; Cytiva) supplemented with 10% fetal bovine serum (cat. no. A6901FBS-500; Invigentech, Inc.), 100 U/ml penicillin and 100 ng/ml streptomycin (Absin Bioscience, Inc.) at 37˚C in a humidified atmosphere containing 5% CO_2/95% air. Diseased human bronchial epithelial (DHBE) cells, which are immortalized cells from the bronchial tube of a patient with chronic obstructive pulmonary disease, were purchased from Otwo Biotech (Shenzhen), Inc. (cat. no. HTX2551) and were cultured identically to BEAS-2B cells. Subsequently, BEAS-2B, DHBE and pNHBE cells were infected with IAV [H3N2; strain was kindly provided by Professor Yan Liu (Department of Microbiology, Anhui Medical University, Hefei, China), multiplicity of infection (MOI), 2] for 48 h at

37˚C prior to subsequent experiments. Locostatin (50 nM) or SCH772984 (1 μM) was used to pretreat DHBE cells 4 h prior to infection with IAV at 37˚C.

Western blotting. Proteins from cells or the right lung tissues of mice were harvested using RIPA lysis buffer (cat. no. P0013B; Beyotime Institute of Biotechnology) and the BCA kit (cat. no. P0010; Beyotime Institute of Biotechnology) was used to determine the protein concentration. Equal amounts of protein (20 μg) were separated by SDS-PAGE on 12.5% gels (cat. no. PG113, Shanghai Epizyme Biomedical Technology Co., Ltd.) and transferred to 0.45 μm PVDF membranes (cat. no. IPVH00010; MilliporeSigma). Subsequently, 5% skim milk powder (cat. no. BS102-500 g; Biosharp Life Sciences) was used to block the membranes for 1 h at room temperature and 1X TBS-0.05% Tween 20 (TBST; cat. no. 9005-64-5; neoFroxx GmbH) was used to wash the membranes three times (10 min/wash). Subsequently, the membranes were incubated with primary anti-RKIP (1:1,000), anti-CDK4 (1:1,000), anti-NLRP3 (1:1,500), anti-ERK1/2 (1:500), anti-p-ERK1/2 (1:300) and anti-β-actin (1:3,000) antibodies at 4˚C overnight. After washing with 1X TBST three times (10 min/wash), the membranes were incubated with a secondary anti-rabbit IgG, HRP-linked antibody (1:2,500; cat. no. 7074; Cell Signaling Technology, Inc.) for 1 h at room temperature. Signals were detected using the Omni-ECL™ Femto Light Chemiluminescence Kit (cat. no. SQ201; Shangh ai Epizyme Biomedical Technology Co., Ltd.) and Tanon 5200 Multi Chemiluminescent Imaging System (Tanon Science and Technology Co., Ltd.). Densitometric analysis was performed using ImageJ 1.53e software (National Institutes of Health).

Reverse transcription-quantitative PCR (RT-qPCR). RNA was extracted from the cells and mice right lung tissues using Total RNA Isolation Reagent (cat. no. YY101; Shangh ai Epizyme Biomedical Technology Co., Ltd.) and reversed transcribed to cDNA using the Hifair® III 1st Strand cDNA Synthesis SuperMix for qPCR (gDNA digester plus) kit (cat. no. 11141ES60; Shanghai Yeasen Biotechnology Co., Ltd.) according to the manufacturer's protocol. qPCR was performed using 2X S6 Universal SYBR qPCR Mix (cat. no. Q204; EnzyArtisan) under the following conditions: 95˚C for 30 sec, followed by 45 cycles at 95˚C for 10 sec and 60˚C for 30 sec. The primer sequences are listed in Table I. The expression levels of target mRNA were calculated using the $2^{-\Delta\Delta Cq}$ method (31) relative to the reference gene (β-actin).

Transduction with RKIP lentivirus. A lentiviral vector overexpressing the RKIP gene (LV5-PEBP1) and its empty vector (LV5NC) were commercially constructed and provided by Shanghai GenePharma Co., Ltd. (3rd generation; cat. no. LV2021-7006). The sequence (Fig. S1) and the shuttle plasmid (Fig. S2) were synthesized by Shanghai GenePharma Co., Ltd. Briefly, 5 μg overexpression vector and the packing vectors, 3 μg PG-P1-VSVG, 2 μg PG-P2-REV and 6 μg PG-P3-RRE, were mixed for 20 min at room temperature to form the transfection mixture and were then co-transfected into 293T cells (80% confluence; cat. no. SCSP-502; Cell Bank of the Chinese Academy of Sciences) using RNAi-Mate (cat. no. G04001; Shanghai GenePharma Co., Ltd.) at 37˚C for 6 h. Subsequently, the transfection complex was removed and fresh medium was added to the cells. The viral supernatant was harvested after 72 h and centrifuged at 20,000 x g for 2 h at 4˚C. The titer of lentivirus was determined by counting GFP-positive cells to determine successfully infected 293T cells. The NC lentivirus was constructed using the same method. Subsequently, BEAS-2B cells were transduced with lentivirus (MOI, 10) and polybrene (5 μg/ml) for 24 h at 37˚C in a humidified atmosphere containing 5% CO_2/95% air, after which, fresh medium was added to the cells. After 3 days, transduction efficiency was observed. The time interval between transfection and subsequent experiments was ≥10 days. BEAS-2B cells infected with the lentivirus were selected with 2 μg/ml puromycin (cat. no. GCD0289949; Shanghai GeneChem Co., Ltd.).

Table I. Primers used for reverse transcription-quantitative PCR.

Primer	Sequence, 5'-3'
RKIP (human) F	GCTCTACACCTTGGTCCTGACA
RKIP (human) R	AATCGGAGAGGACTGTGCCACT
IL-1β (human) F	CCACAGACCTTCCAGGAGAATG
IL-1β (human) R	GTGCAGTTCAGTGATCGTACAGG
IL-18 (human) F	AGCAAGGAATTGTCTCCCAG
IL-18 (human) R	GAAGCGATCTGGAAGGTCTG
β-actin (human) F	CACCATTGGCAATGAGCGGTTC
β-actin (human) R	AGGTCTTTGCGGATGTCCACGT
IL-1β (mouse) F	TGGACCTTCCAGGATGAGGACA
IL-1β (mouse) R	GTTCATCTCGGAGCCTGTAGTG
IL-18 (mouse) F	AGGGTTTGTGTTCCAGAAAGATG
IL-18 (mouse) R	AGCCTCGGGTATTCTGTTATGG
β-actin (mouse) F	CATTGCTGACAGGATGCAGAAGG
β-actin (mouse) R	TGCTGGAAGGTGGACAGTGAGG

F, forward; R, reverse; RFIP, Raf kinase inhibitor protein.

Immunofluorescence staining. Cells were plated in 24-well culture plates after 48 h of IAV infection. The cells were then washed with cold phosphate-buffered saline, fixed with 4% paraformaldehyde for 20 min at room temperature and permeabilized with 0.1% Triton X-100 for 15 min at room temperature. After being blocked with 5% BSA (cat. no. 9048-46-8; neoFroxx GmbH) at room temperature for 30 min, the cells were incubated with RKIP antibody (1:100) overnight at 4˚C and were then incubated with Alexa Fluor® 594 goat anti-rabbit IgG H&L (1:500; cat. no. ab150080; Abcam) for 1 h at room temperature. DAPI (cat. no. C1002; Beyotime Institute of Biotechnology) was applied for 15 min in the dark at room temperature to visualize the nuclei, and the cells were detected under a laser confocal microscope (Zeiss LSM880; Carl Zeiss AG).

ELISA. The levels of inflammatory cytokines IL-1β and IL-18 in cellular supernatants were examined using IL-1β (cat. no. ml058059) and IL-18 (cat. no. ml058055) ELISA kits

(all from Shanghai Enzyme-linked Biotechnology Co., Ltd.). The levels of IL-1β and IL-18 in the serum and bronchoalveolar lavage fluid (BALF) of mice were measured using IL-1β (cat. no. ml301814) and IL-18 (cat. no. ml002294) (all from Shanghai Enzyme-linked Biotechnology Co., Ltd.). ELISA kits were performed according to the manufacturer's protocols.

Cell cycle assay. Cells ($1x10^5$/well) were plated in 12-well plates and were fixed in 70% ethanol at 4˚C overnight. The cells were then stained with propidium iodide/RNase A (cat. no. C1052; Beyotime Institute of Biotechnology) at 37˚C for 30 min in the dark. Cell cycle progression was assessed using a NovoCyte flow cytometer (Agilent Technologies, Inc.) and FlowJo software (FlowJo X 10.0.7r2; FlowJo LLC).

Cell viability assay. Cells were plated at a density of $5x10^3$ in 96-well plates. After cells were infected with IAV (MOI, 2) for 48 h at 37˚C in a humidified atmosphere containing 5% CO_2, cell viability was assessed using a Cell Counting Kit-8 (CCK-8) kit (cat. no. C0037; Beyotime Institute of Biotechnology) according to the manufacturer's instructions. Briefly, 10 μl CCK-8 reagent was added to each well, and the cells were incubated at 37˚C for 2 h. Absorbance was measured at 450 nm to evaluate cell viability.

5-Ethynyl-2'-deoxyuridine (EdU) assay. Cells ($2x10^4$/well) were cultured in 24-well plates after IAV infection for 48 h and an EdU kit (cat. no. C0075S; Beyotime Institute of Biotechnology) was used to detect the degree of DNA damage according to the manufacturer's protocol. Briefly, 10 μM EdU was used to incubate cells at 37˚C for 2 h to label them. Subsequently, cells were fixed in 4% paraformaldehyde at room temperature for 20 min and permeabilized with 0.1% Triton X-100 at room temperature for 15 min. Next, cells were dyed with reaction solution for 30 min at room temperature in the dark and the Hoechst was applied for 15 min at room temperature in dark. The results were analyzed using a Leica fluorescence microscope (Leica DM6B; Leica Microsystems, Inc.).

Hematoxylin and eosin (H&E) staining. Lung tissues harvested in animal experiments were fixed in 4% paraformaldehyde at room temperature for 48 h, embedded in paraffin, cut into 5-μm sections and stained using a H&E stain kit (cat. no. G1120; Beijing Solarbio Science & Technology Co., Ltd.). Briefly, the sections were stained with hematoxylin solution for 10 min at room temperature and washed in running tap water for 5 min, after which, differentiation solution was added for 10 sec at room temperature. The sections were subsequently stained with eosin solution for 10 sec at room temperature, dehydrated in alcohol (75, 85, 95 and 100%; each for 2-3 sec at room temperature) and rinsed in 100% alcohol for 1 min at room temperature. After clearing with xylene and sealing with neutral balsam, the sections were scanned using a Pannoramic Whole Slide Scanner (Pannoramic Desk; 3DHISTECH Kft.) and viewed with Caseviewer 2.2 (3DHISTECH Kft.). Histological scores of inflammation in the lungs of IAV-induced mice were semi-quantified using the following scoring system: 0, no inflammation; 1, only moderate peribronchial inflammation; 2, <10% inflamed lung tissue; 3, 10-25% inflamed lung tissue; 4, 26-50% inflamed lung tissue; 5, >50% inflamed lung tissue (32). Scoring was performed independently by two investigators, whose scores were averaged.

Immunohistochemistry (IHC). Briefly, lung tissues were fixed, embedded and sectioned as performed prior to H&E staining. The sections were then deparaffinized in xylene, rehydrated in a graded series of alcohol and subjected to antigen retrieval by microwaving (650 W) for 12 min in sodium citrate buffer (pH 6.0). The endogenous peroxidase activity was quenched by incubating the sections in 3% H_2O_2 for 15 min at room temperature. Subsequently, the lung tissue sections were blocked with 5% BSA for 30 min at room temperature and then incubated with RKIP primary antibody (1:250) at 4˚C overnight, after which they were incubated with a goat anti-rabbit IgG H&L (HRP) secondary antibody (1:1,000; cat. no. ab97051; Abcam) at room temperature for 1 h. After DAB staining for 25 sec at room temperature, the sections were counterstained with hematoxylin and dyed in 1% ammonia solution for 30 sec at room temperature. The sections were scanned using a Pannoramic Whole Slide Scanner (Pannoramic Desk) and viewed with Caseviewer 2.2.

Statistical analysis. For *in vitro* experiments, each measurement was obtained by three independent experiments. The data are presented as the mean ± SEM and statistical analyses were conducted using SPSS 23.0 (IBM, Corp.). Differences between two groups were analyzed using unpaired Student's t-test, whereas differences among three or more groups were assessed by one-way ANOVA and Tukey's post hoc test. The histological score was presented as median and IQR, and was statistically analyzed using Kruskal-Wallis and Dunn's post hoc test. $P<0.05$ was considered to indicate a statistically significant difference.

Results

Effects of IAV infection on the expression of RKIP in BEAS-2B, DHBE and pNHBE cells. BEAS-2B and DHBE cells were exposed to IAV (MOI, 2) for 48 h and the expression levels of RKIP were detected. Notably, the expression levels of RKIP were significantly decreased following IAV infection in both BEAS-2B cells ($P=0.0083$; Fig. 1A and B) and DHBE cells ($P<0.0001$; Fig. 1E and F), as assessed by western blotting. Subsequently, inflammatory cytokines were assessed using RT-qPCR and ELISA; the results revealed that IL-1β and IL-18 were significantly increased in response to IAV (MOI, 2) infection for 48 h in BEAS-2B cells, as determined by RT-qPCR ($P<0.0001$ for IL-1β, $P=0.0081$ for IL-18; Fig. 1C) and ELISA ($P<0.0001$ for IL-1β, $P=0.0035$ for IL-18; Fig. 1D). Similarly, IL-1β and IL-18 levels were elevated in DHBE cells in response to IAV, as determined using RT-qPCR ($P=0.0010$ for IL-1β, $P=0.0029$ for IL-18; Fig. 1G) and ELISA ($P=0.0016$ for IL-1β, $P=0.0005$ for IL-18; Fig. 1H). To further confirm this result, pNHBE cells were employed to detect the levels of RKIP and inflammatory cytokines. As shown in Fig. 1I and J ($P=0.0100$), RKIP was significantly reduced in pNHBE cells after IAV infection (MOI, 2), as determined by western blotting; by contrast, IL-1β and IL-18 were increased,

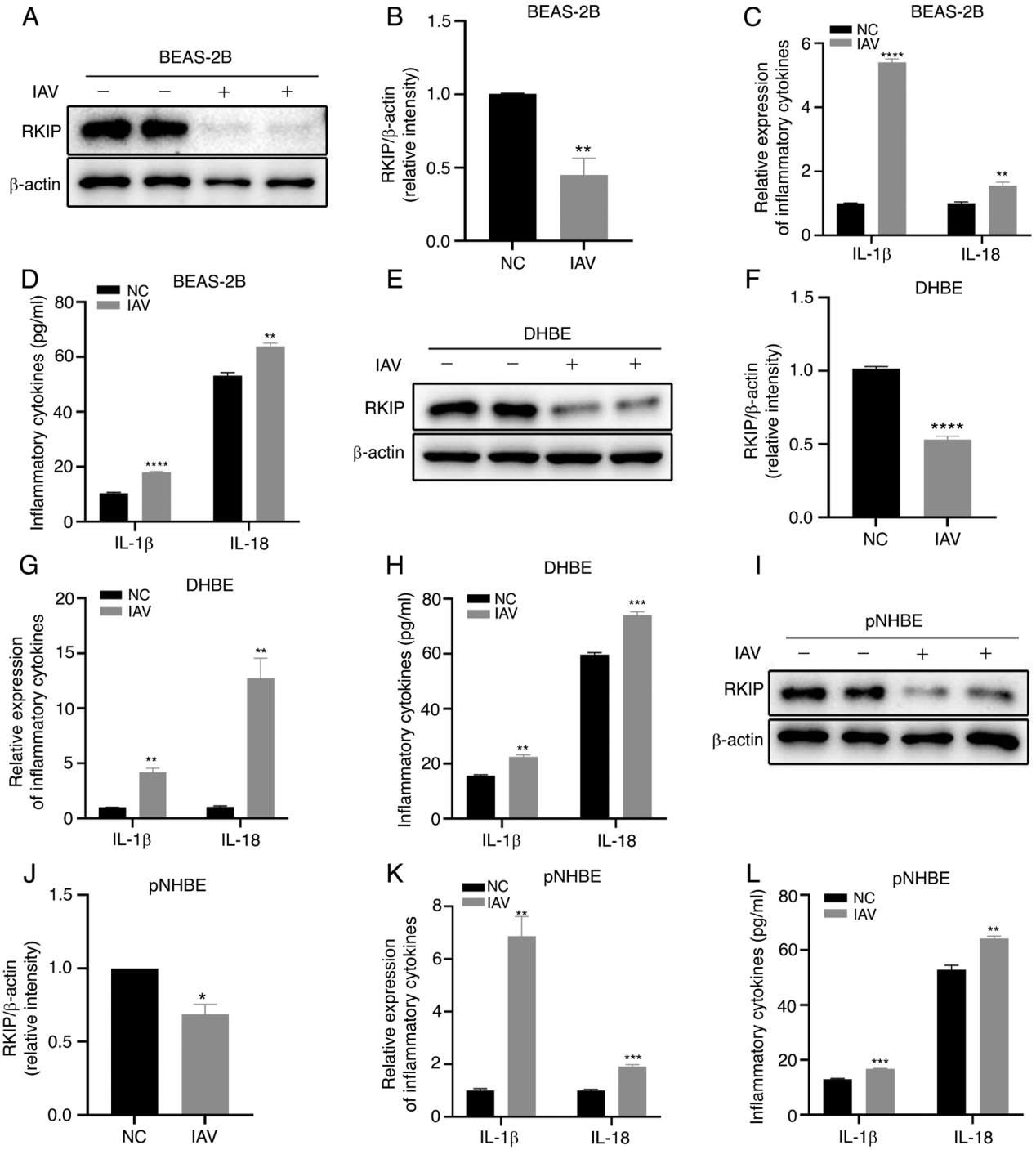

Figure 1. Effects of IAV infection (multiplicity of infection, 2) for 48 h on BEAS-2B, DHBE and pNHBE cells. (A and B) Protein expression levels of RKIP in BEAS-2B cells. (C) mRNA expression levels of IL-1β and IL-18 in BEAS-2B cells were detected by RT-qPCR. (D) Levels of IL-1β and IL-18 in BEAS-2B cells were detected by ELISA. (E and F) Protein expression levels of RKIP in DHBE cells. (G) mRNA expression levels of IL-1β and IL-18 in DHBE cells. (H) Levels of IL-1β and IL-18 in DHBE cells were detected by ELISA. (I and J) Protein expression levels of RKIP in pNHBE cells were detected by western blotting. (K) mRNA expression levels of IL-1β and IL-18 in pNHBE cells were detected by RT-qPCR. (L) Levels of IL-1β and IL-18 in pNHBE cells were detected by ELISA. *P<0.05, **P<0.01, ***P<0.001 and ****P<0.0001 vs. NC. DHBE, diseased human bronchial epithelial; IAV, influenza A virus; NC, negative control; pNHBE, primary human bronchial epithelial; RKIP, Raf kinase inhibitor protein; RT-qPCR, reverse transcription-quantitative PCR.

as revealed by RT-qPCR (P=0.0015 for IL-1β, P=0.0004 for IL-18; Fig. 1K) and ELISA (P=0.0005 for IL-1β, P=0.0034 for IL-18; Fig. 1L). These results indicated that IAV infection significantly attenuated RKIP expression in BEAS-2B, DHBE and pNHBE cells, and that the airway inflammatory cytokines, IL-1β and IL-18, were significantly elevated in response to IAV infection.

RKIP inhibition by locostatin augments inflammatory responses induced by IAV in airway epithelial cells. To investigate whether airway inflammation induced by IAV was regulated by RKIP, the DHBE cells were pretreated for 4 h before IAV infection with locostatin. Locostatin is a small molecule that covalently binds RKIP, which results in a protein-protein interaction where locostatin inhibits

and abrogates the ability of RKIP to bind; locostatin also inhibits Raf-1 kinase specifically to inhibit the expression of RKIP (33,34). The present study ascertained that the expression of RKIP was significantly reduced in the IAV(+) + locostatin(+) group compared with in the IAV(+) + locostatin(-) group, as determined using western blotting (P=0.0003; Fig. 2A and B) and immunofluorescence (Fig. 2J). In addition, the mRNA expression levels of the inflammatory cytokines IL-1β and IL-18 were detected by RT-qPCR and the cellular supernatant levels were detected by ELISA. As shown in Fig. 2F and G, the mRNA expression levels of the cytokines were elevated in the IAV(+) + locostatin(-) group compared with in the NC group (P=0.0107 for IL-1β, P=0.0016 for IL-18) and were more markedly increased in the IAV(+) + locostatin(+) group compared with in the IAV(+) + locostatin(-) group (P=0.0004 for IL-1β, P=0.0046 for IL-18). As shown in Fig. 2H and I, ELISA exhibited similar trends to RT-qPCR; IL-1β and IL-18 were significantly elevated in the IAV(+) + locostatin(-) group compared with in the NC group (P=0.0002 for IL-1β, P=0.0002 for IL-18) and were more markedly increased in the IAV(+) + locostatin(+) group compared with in the IAV(+) + locostatin(-) group (P=0.0010 for IL-1β, P=0.0198 for IL-18). Furthermore, the protein expression levels of NLRP3 also exhibited a similar trend, as determined using western blotting [P=0.0002 for IAV(+) + locostatin(-) group vs. IAV(-) + locostatin(-) group; P=0.0094 for IAV(+) + locostatin(+) group vs. IAV(+) + locostatin(-) group; Fig. 2A and C). To further confirm the effect of RKIP on cell cycle progression in DHBE cells, western blotting was performed and revealed that CDK4 was downregulated after IAV infection compared with in the NC group (P=0.0489), and the same trend was observed in the IAV(+) + locostatin(+) group compared with in the IAV(+) + locostatin(-) group (P=0.0052) (Fig. 2A and D). Additionally, the EdU (Fig. 2K and L) and CCK-8 (Fig. 2M) assays confirmed that there was enhanced DNA damage and reduced cell viability in the IAV(+) + locostatin(+) group compared with in the IAV(+) + locostatin(-) group (P=0.0351 for EdU, P<0.0001 for CCK-8) and the IAV(+) + locostatin(-) group compared with in the NC group (P=0.0021 for EdU, P=0.0007 for CCK-8). Furthermore, the cell cycle was analyzed using flow cytometry. As shown in Fig. 2N and O, there was a significant inhibition in the number of cells at S phase in the IAV(+) + locostatin(-) group compared with in the NC group (P=0.0004). Furthermore, the G_1 phase of cell cycle was arrested (P=0.0488) and the ratio of S phase was decreased in the IAV(+) + locostatin(+) group compared with in the IAV(+) + locostatin(-) group (P=0.0021). Furthermore, the protein expression levels of ERK1/2 and p-ERK1/2 were detected using western blotting (Fig. 2A and E). The results suggested that the ratio of pERK1/2/ERK1/2 was increased when comparing the IAV(+) + locostatin(-) group with the NC group (P=0.0106), and the IAV(+) + locostatin(+) group with the IAV(+) + locostatin(-) group (P=0.0224). These results suggested that the inhibition of RKIP by locostatin may increase the inflammatory response and suppress cell cycle progression during the inflammatory response induced by IAV.

RKIP alleviates the inflammatory response in BEAS-2B cells after IAV infection. To further confirm that RKIP regulated inflammation and cell cycle progression after IAV infection, RKIP overexpression (RKIP-OE) was induced in BEAS-2B cells by lentiviral transduction. As shown in Fig. 3B, the mRNA expression levels of RKIP were significantly upregulated after transduction, as determined by RT-qPCR (P=0.0021). As shown in Fig. 3A, C and K, the expression levels of RKIP were markedly reduced after IAV infection, as detected by western blotting (P=0.0037) and immunofluorescence. Furthermore, changes in the inflammatory protein NLRP3 were determined through western blotting and it was demonstrated that RKIP-OE significantly alleviated the inflammatory response after IAV infection (P=0.0323; Fig. 3A and D). Furthermore, the inflammatory cytokines, IL-1β and IL-18, were assessed and it was revealed that their levels were significantly increased in the IAV(+) + RKIP-OE(-) group compared with in the NC group by RT-qPCR (P=0.0057 for IL-1β, P=0.0061 for IL-18; Fig. 3G and H) and ELISA (P=0.0008 for IL-1β, P=0.0009 for IL-18; Fig. 3I and J). By contrast, the levels of IL-1β and IL-18 were significantly inhibited in the IAV(+) + RKIP-OE(+) group compared with in the IAV(+) + RKIP-OE(-) group, as determined by RT-qPCR (P=0.0337 for IL-1β, P=0.0287 for IL-18; Fig. 3G and H) and ELISA (P=0.0110 for IL-1β, P=0.0006 for IL-18; Fig. 3I and J). The present study also assessed CDK4 expression, as it is related to the cell cycle; the western blotting results revealed that CDK4 was upregulated when RKIP was overexpressed after IAV infection (P=0.0212; Fig. 3A and E). In addition, cell cycle progression was impaired after IAV infection in BEAS-2B cells; however, RKIP-OE reversed this effect, as reflected by the results of EdU (P=0.0236; Fig. 3L and M) and CCK-8 (P=0.0090; Fig. 3N) assays. Flow cytometry of cell cycle kinetics suggested that the G_1 phase of cell cycle was arrested (P=0.0011) and the ratio of S stage was decreased in the IAV(+) + RKIP-OE(-) group compared with in the NC group (P<0.0001; Fig. 3O and P), and that the percentage of cells in S phase that was reduced after IAV infection was restored when RKIP was overexpressed (P=0.0048; Fig. 3O and P). RKIP-OE significantly mitigated the production of inflammatory cytokines and provided recovery from cell cycle arrest in BEAS-2B cells following IAV infection. Furthermore, overexpression of RKIP decreased the ratio of p-ERK1/2/ERK1/2 induced by IAV infection, as determined by western blotting (P=0.0403; Fig. 3A and F). All of these results revealed that OE of RKIP alleviated the inflammatory response and restored cell cycle progression in BEAS-2B cells infected with IAV.

RKIP regulates the inflammatory response via the ERK/MAPK pathway. To investigate whether RKIP regulated the inflammatory response via the ERK/MAPK pathway, the specific ERK/MAPK-pathway inhibitor SCH772984 was used to treat cells after challenging them with or without IAV. The protein expression levels of RKIP, ERK1/2 and p-ERK1/2 were determined by western blotting, and the results suggested that SCH772984 significantly inhibited the ERK/MAPK pathway as p-ERK1/2/ERK1/2 was reduced in response to the IAV(-) + SCH772984(+) + locostatin(-) group compared with the IAV(-) + SCH772984(-) + locostatin(-) group (P=0.0416; Fig. 4A and C). In addition, SCH772984 reversed activation of the ERK/MAPK pathway induced by IAV and RKIP inhibition, as determined by comparing the IAV(+) + SCH772984(+) + locostatin(+) group with the IAV(+) + SCH772984(-) +

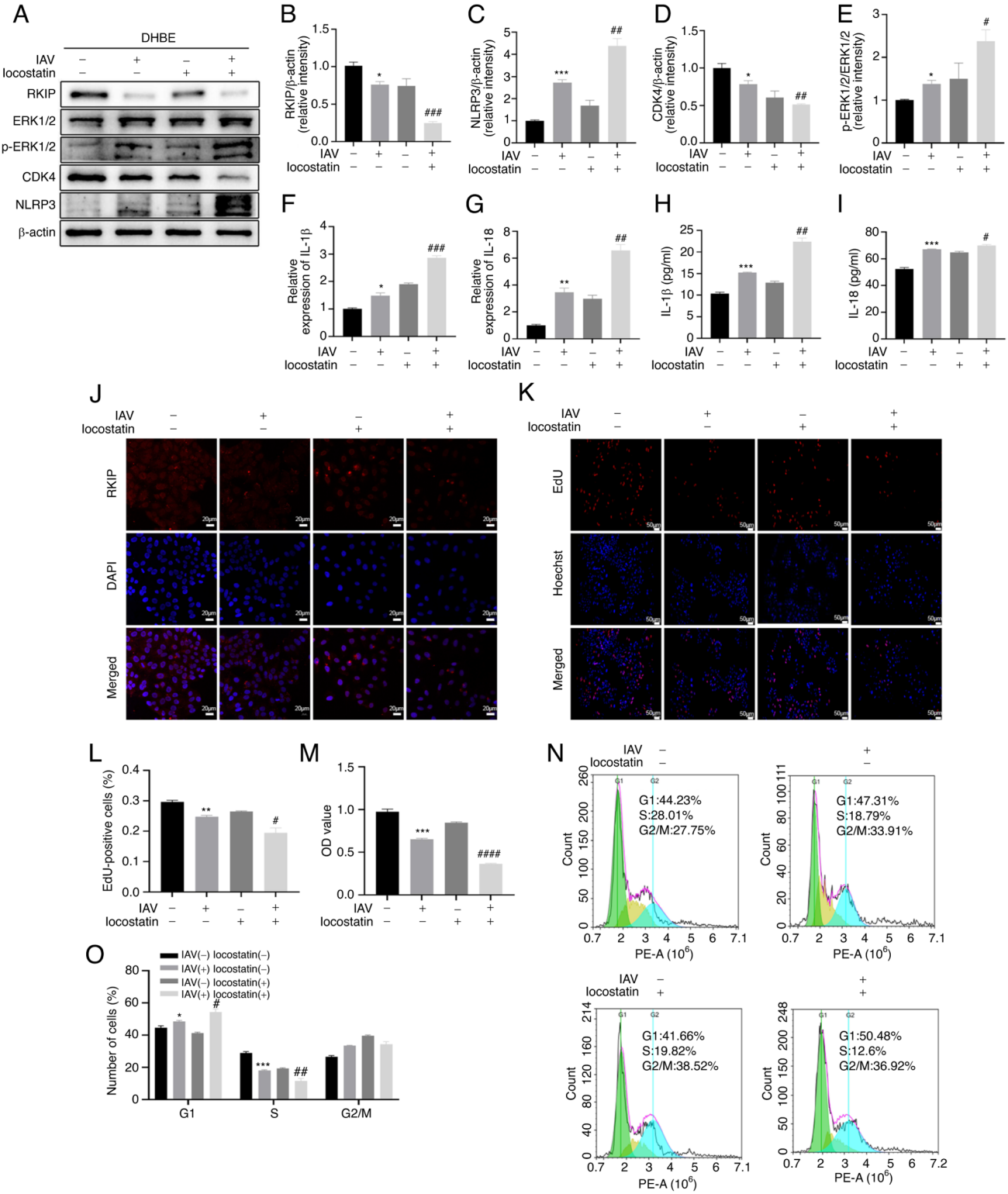

Figure 2. RKIP inhibition by locostatin (50 nM) augments inflammatory responses induced by IAV infection (multiplicity of infection, 2) for 48 h in DHBE cells. (A) Protein expression levels of RKIP, ERK1/2, p-ERK1/2, CDK4 and NLRP3 were detected by western blotting. Densitometric analysis of (B) RKIP, (C) NLRP3, (D) CDK4 and (E) p-ERK1/2 normalized to ERK1/2 in the different groups. (F and G) mRNA expression levels of the inflammatory cytokines IL-1β and IL-18 were measured by reverse transcription-quantitative PCR. (H and I) Levels of the inflammatory cytokines IL-1β and IL-18 were measured by ELISA. (J) Immunofluorescence staining was performed to detect the expression of RKIP. RKIP (red) and DAPI (blue); scale bars, 20 μm; magnification, x200. (K and L) EdU assay was used to detect cells synthesizing DNA in the S phase of the cell cycle. Scale bar, 50 μm; magnification, x50. (M) Cell Counting Kit-8 was used to detect the viability of DHBE cells. (N and O) Cell cycle was detected by flow cytometry. *P<0.05, **P<0.01 and ***P<0.001 vs. NC; $^{\#}$P<0.05, $^{\#\#}$P<0.01, $^{\#\#\#}$P<0.001 and $^{\#\#\#\#}$P<0.0001 vs. IAV(+) + locostatin(-). DHBE, diseased human bronchial epithelial; EdU, 5-ethynyl-2'-deoxyuridine; IAV, influenza A virus; NC, negative control; NLRP3, NLR family pyrin domain-containing 3; p, phosphorylated; RKIP, Raf kinase inhibitor protein.

locostatin(+) group (P=0.0182; Fig. 4A and C). Following IAV infection, IL-1β and IL-18 levels were elevated compared with in the control group (P=0.0297 for IL-1β, P=0.0093 for IL-18), and their levels were significantly increased in

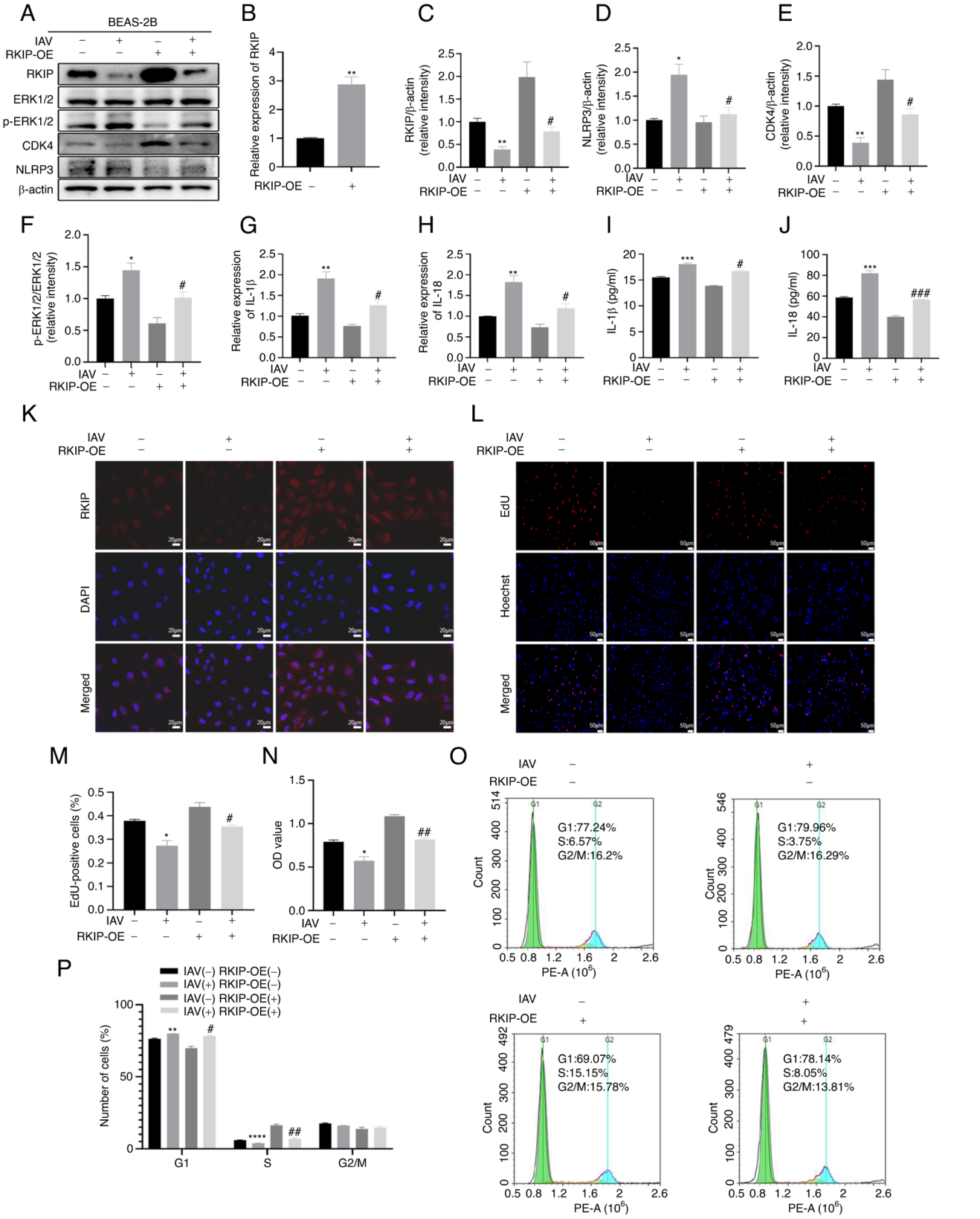

Figure 3. RKIP alleviates the inflammatory response in BEAS-2B cells after IAV infection. (A) Protein expression levels of RKIP, ERK1/2, p-ERK1/2, CDK4 and NLRP3 in BEAS-2B cells were detected by western blotting. Densitometric analysis of (C) RKIP, (D) NLRP3, (E) CDK4 and (F) p-ERK1/2 normalized to ERK1/2 in the different groups. (B) Efficiency of RKIP-OE lentivirus transduction was verified in BEAS-2B cells by RT-qPCR. (G and H) mRNA expression levels of the inflammatory cytokines IL-1β and IL-18 were measured by RT-qPCR. (I and J) Levels of the inflammatory cytokines IL-1β and IL-18 were measured by ELISA. (K) Immunofluorescence staining was performed to detect the expression of RKIP. RKIP (red) and DAPI (blue); scale bar, 20 μm; magnification, x200. (L and M) EdU assay was used to detect the cells synthesizing DNA in the S-phase of the cell cycle. Scale bar, 50 μm; magnification, x50. (N) Cell Counting Kit-8 was used to detect the viability of BEAS-2B cells. (O and P) Cell cycle was detected by flow cytometry. *P<0.05, **P<0.01, ***P<0.001 and ****P<0.0001 vs. NC; $^{\#}$P<0.05, $^{\#\#}$P<0.01 and $^{\#\#\#}$P<0.001 vs. IAV(+) + RKIP-OE(-). EdU, 5-ethynyl-2'-deoxyuridine; IAV, influenza A virus; NC, negative control; NLRP3, NLR family pyrin domain-containing 3; OE, overexpression; p, phosphorylated; RKIP, Raf kinase inhibitor protein; RT-qPCR, reverse transcription-quantitative PCR.

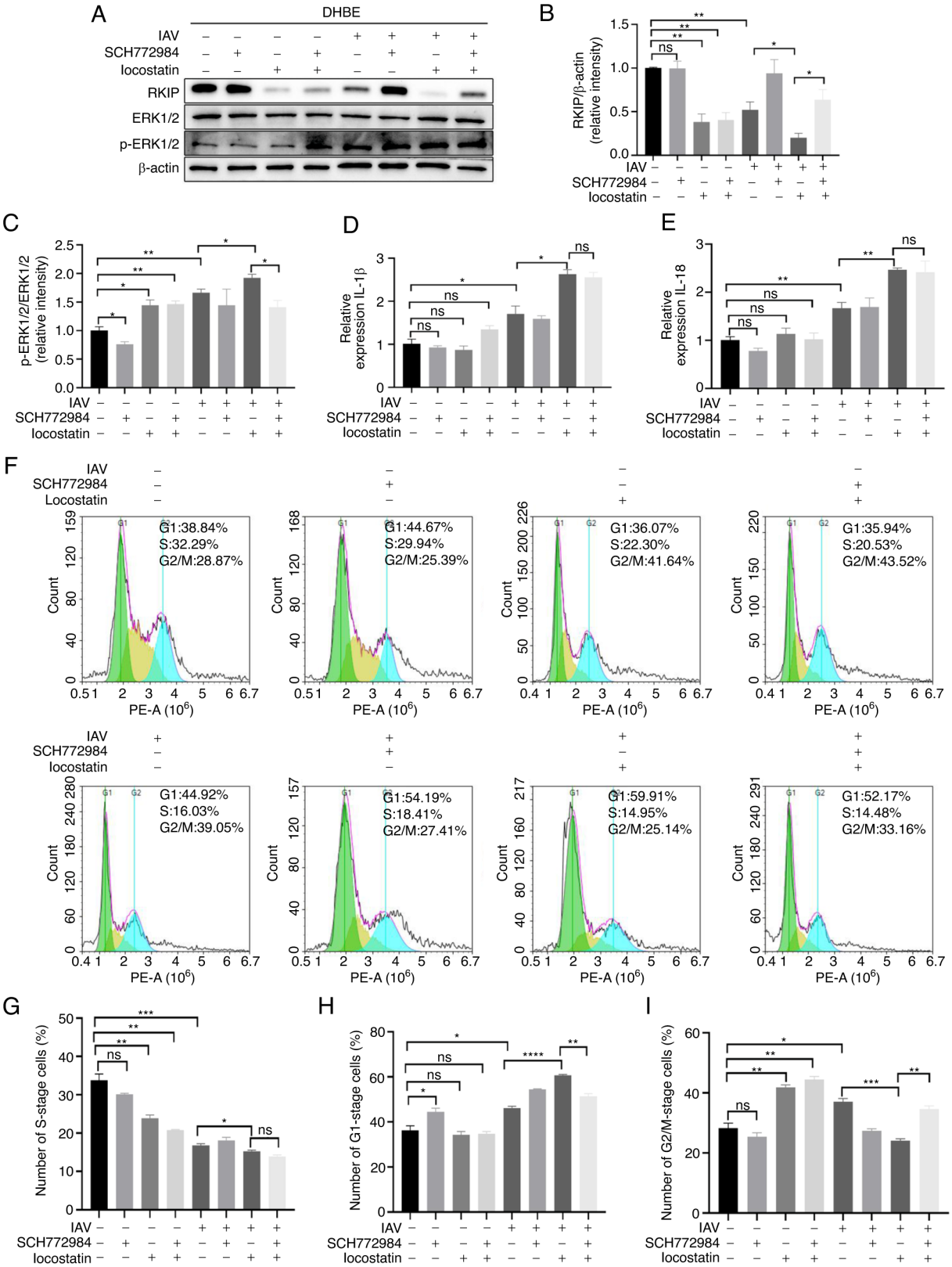

Figure 4. RKIP regulates the inflammatory response via the ERK/MAPK pathway. (A) Protein expression levels of RKIP, ERK1/2 and p-ERK1/2 in DHBE cells were detected by western blotting. Densitometric analysis of (B) RKIP and (C) p-ERK1/2 normalized to ERK1/2 in the different groups. (D and E) mRNA expression levels of the inflammatory cytokines IL-1β and IL-18 were measured by reverse transcription-quantitative PCR. (F-I) Number of cells in S stage, G_1 stage and G_2/M stage of the cell cycle was detected by flow cytometry. *P<0.05, **P<0.01, ***P<0.001 and ****P<0.0001. DHBE, diseased human bronchial epithelial; IAV, influenza A virus; ns, not significant (P>0.05); p, phosphorylated; RKIP, Raf kinase inhibitor protein.

the IAV(+) + SCH772984(-) + locostatin(+) group compared with in the IAV(+) + SCH772984(-) + locostatin(-) group (P=0.0122 for IL-1β, P=0.0033 for IL-18), as determined using RT-qPCR (Fig. 4D and E). In addition, when the ERK/MAPK

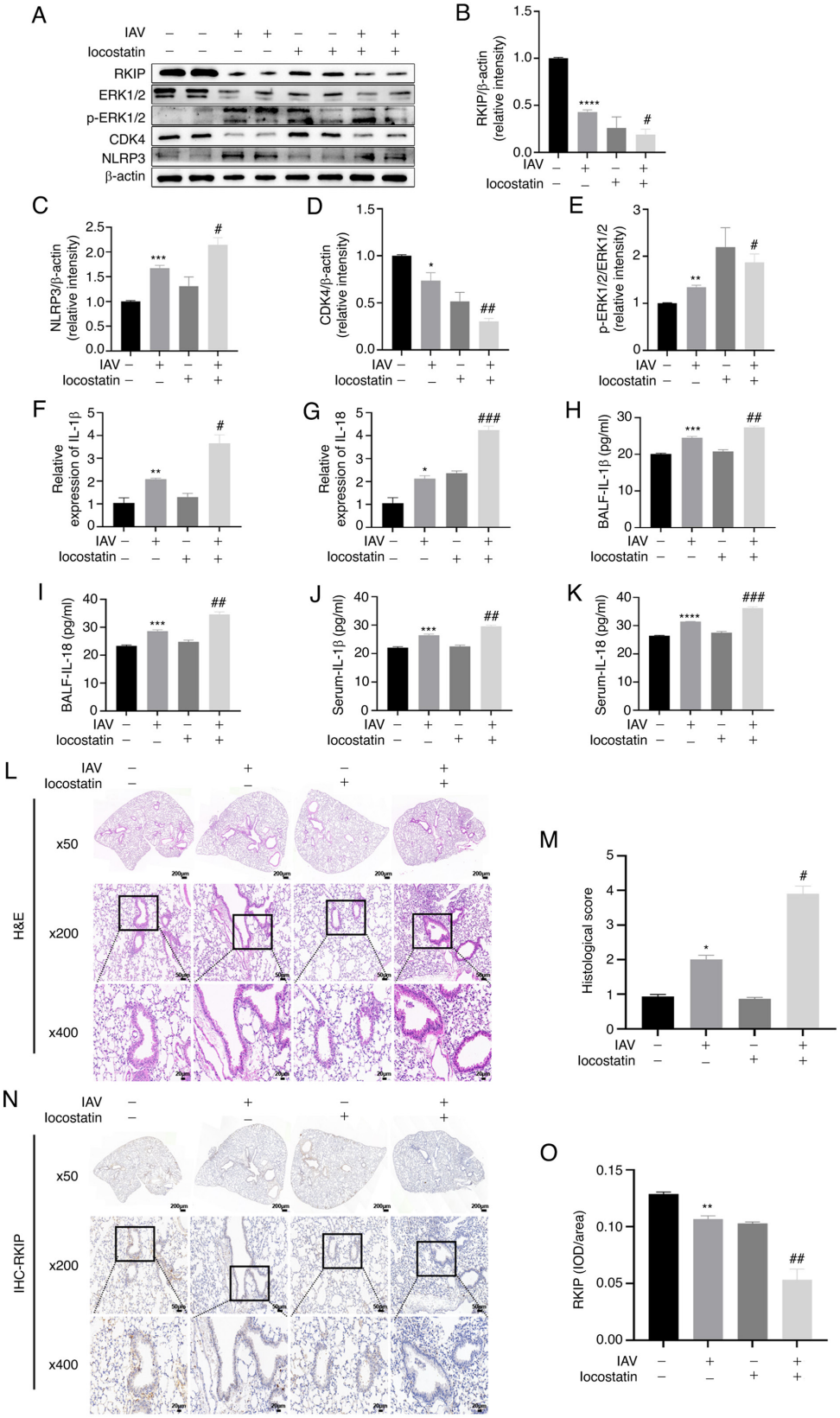

Figure 5. Inhibition of RKIP aggravates the airway inflammatory response *in vivo*. After locostatin (10 mg/kg) was administered by intraperitoneal injection, mice were treated with 0.9% saline or 100 μl IAV in saline via oropharyngeal aspiration. (A) Lung tissues were harvested to detect the protein expression levels of RKIP, ERK1/2, p-ERK1/2, NLRP3 and CDK4 by western blotting. Densitometric analysis of (B) RKIP, (C) NLRP3, (D) CDK4 and (E) p-ERK1/2 normalized to ERK1/2 in the different groups. (F and G) Lung tissues were harvested to detect the mRNA expression levels of IL-1β and IL-18 by reverse transcription-quantitative PCR. (H and I) BALF and (J and K) serum were harvested to examine the levels of the inflammatory cytokines IL-1β and IL-18 by ELISA. (L and M) H&E staining was used to evaluate the semi-quantitative scoring of inflammation in lung tissue. Scale bar, 200 μm for magnification x50; 50 μm for magnification x200; 20 μm for magnification x400. (N and O) IHC was performed to localize RKIP in bronchial epithelium. Scale bar, 200 μm for magnification x50; 50 μm for magnification x200; 20 μm for magnification x400. *P<0.05, **P<0.01, ***P<0.001 and ****P<0.0001 vs. NC; $^{\#}$P<0.05, $^{\#\#}$P<0.01 and $^{\#\#\#}$P<0.001 vs. IAV(+) + locostatin(-). BALF, bronchoalveolar lavage; H&E, hematoxylin and eosin; IAV, influenza A virus; IHC, immunohistochemistry; IOD, integrated optical density; NLRP3, NLR family pyrin domain-containing 3; p, phosphorylated; RKIP, Raf kinase inhibitor protein.

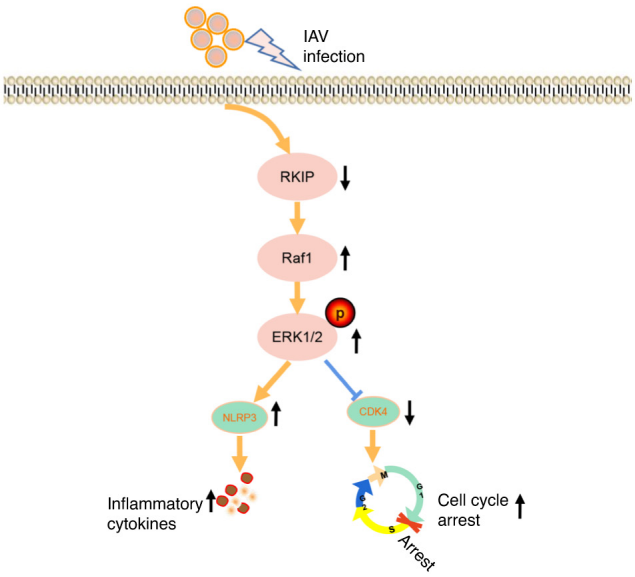

Figure 6. Schematic elucidation of the possible mechanism of RKIP in IAV-induced airway inflammatory response via the ERK/MAPK pathway. IAV, influenza A virus; NLRP3, NLR family pyrin domain-containing 3; p, phosphorylated; RKIP, Raf kinase inhibitor protein.

pathway was inhibited by SCH772984, inhibiting RKIP did not induce a significant change in the inflammatory cytokines IL-1β and IL-18, as determined by RT-qPCR (Fig. 4D and E). Cells were arrested in G_1 phase (P=0.0106; Fig. 4H) and the proportion of cells in S phase was decreased after IAV infection (P=0.0006; Fig. 4G) when comparing the IAV(+) + SCH772984(-) + locostatin(-) group with the IAV(-) + SCH772984(-) + locostatin(-) group, and locostatin aggravated the effects of IAV infection (P<0.0001 for G_1 phase, P=0.0325 for S phase) when comparing the IAV(+) + SCH772984(-) + locostatin(+) group with the IAV(+) + SCH772984(-) + locostatin(-) group. However, there was no significant difference in the percentage of cells in S phase in the IAV(+) + SCH772984(+) + locostatin(+) group compared with in the IAV(+) + SCH772984(-) + locostatin(+) group, as determined using flow cytometry (P>0.05; Fig. 4F and G). These results suggested that the percentage of cells in S phase were not influenced when SCH772984 was used to inhibit the ERK/MAPK pathway, even after inhibiting RKIP. As shown in Fig. 4F, H and I, there were significant differences in the number of cells at G_1 (P=0.0016) and G_2/M (P=0.0010) phases in the IAV(+) + SCH772984(+) + locostatin(+) group compared with in the IAV(+) + SCH772984(-) + locostatin(+) group. This confirmed that RKIP regulated inflammatory cytokine levels and the S phase of cell cycle progression via the ERK/MAPK signal transduction pathway.

Inhibition of RKIP aggravates the airway inflammatory response in vivo. To further confirm the effects of RKIP *in vivo*, a mouse model infected with IAV was implemented. In our previous study (29), a model of airway inflammation was established and changes in the inflammatory cytokines IL-1β and IL-18, related protein expression and histopathology were analyzed 7 days after IAV infection. BALF and serum were collected to examine the IL-1β and IL-18 levels, and it was revealed that the levels of these two cytokines were significantly increased in the BALF (P=0.0006 for IL-1β, P=0.0009 for IL-18; Fig. 5H and I) and serum (P=0.0009 for IL-1β, P<0.0001 for IL-18; Fig. 5J and K) of the IAV(+) + locostatin(-) group compared with in the NC group, as determined by ELISA. The levels of IL-1β and IL-18 were also significantly elevated in the BALF (P=0.0064 for IL-1β, P=0.0042 for IL-18; Fig. 5H and I) and serum (P=0.0049 for IL-1β, P=0.0003 for IL-18; Fig. 5J and K) in the IAV(+) + locostatin(+) group compared with in the IAV(+) + locostatin(-) group, as determined using ELISA. Furthermore, the mRNA expression levels of IL-1β and IL-18 were detected in lung tissues, and it was revealed that trends in IL-1β and IL-18 lung tissue expression were similar to those in BALF and serum (Fig. 5F and G). These findings indicated that the expression levels of IL-1β and IL-18 were augmented after IAV infection (P=0.0100 for IL-1β, P=0.0179 for IL-18), and that the inhibition of RKIP exacerbated the production of IL-1β and IL-18 after IAV infection (P=0.0134 for IL-1β, P=0.0006 for IL-18). In addition, the protein expression levels of NLRP3 were detected using western blotting. As shown in Fig. 5A and C, IAV infection increased the expression levels of NLRP3 (P=0.0004) and locostatin exacerbated this increase (P=0.0360). IAV-induced histopathological changes in the lung were also assessed. As shown in Fig. 5L and M, more severe infiltration of inflammation was observed in IAV-infected mice compared with in the control group (P=0.0113). Furthermore, locostatin increased the pulmonary inflammation of mice infected with IAV (P=0.048). To further determine the expression of RKIP in lung tissues from C57BL/6 mice, the expression levels of RIKP were assessed by western blotting and IHC. As shown in Fig. 5A, B, N and O, RKIP was significantly attenuated in response to IAV (P<0.0001 for western blotting, P=0.0026 for IHC) and locostatin (P=0.0169 for western blotting, P=0.0057 for IHC) further decreased RKIP expression. ERK1/2 and p-ERK1/2 expression levels were also detected, in order to determine whether the ERK/MAPK pathway was activated, and CDK4 expression was measured to assess the cell cycle, using western blotting (Fig. 5A, D and E); notably, IAV activated the ERK/MAPK pathway (P=0.0017) and the expression of CDK4 was significantly decreased (P=0.0374) compared with in the control group. Furthermore, RKIP inhibition by locostatin aggravated these effects (P=0.0464 for p-ERK1/2/ERK1/2, P=0.0090 for CDK4/β-actin), thus suggesting that RKIP may be a negative regulator of IAV-induced airway inflammatory responses.

Discussion

The present study demonstrated that RKIP functions as an inhibitory mediator of IAV-induced airway inflammatory response, and that it acts via the ERK/MAPK pathway. RKIP-OE significantly mitigated the production of inflammatory cytokines and reversed the cell cycle arrest triggered by IAV infection. To the best of our knowledge, the present study is the first to demonstrate that the RKIP-mediated, IAV-induced airway inflammatory response is conducted via the ERK/MAPK pathway *in vitro* and *in vivo*.

While RKIP has been reported to be involved in numerous disease processes (17,21,35), the role of RKIP in the airway inflammatory response induced by IAV remains to be

elucidated. The present study ascertained that the expression of RKIP was downregulated in BEAS-2B, DHBE and pNHBE cells following IAV infection, whereas the levels of the inflammatory cytokines IL-1β and IL-18 were elevated. These results suggested that RKIP was critical to the airway inflammatory response following IAV infection.

The present study further investigated the role of RKIP in airway inflammatory responses following IAV infection; notably, it was observed that the expression of RKIP was specifically downregulated by locostatin and that this then exacerbated airway inflammation. The viability and proliferation of cells also slowed with the inhibition of RKIP expression suggesting that RKIP was involved in cell cycle progression. Furthermore, the percentage of cells in S phase of cell cycle was significantly decreased after IAV infection and inhibition of RKIP expression further diminished the proportion of cells in the S phase. Previous reports have also demonstrated the involvement of RKIP in cell cycle progression (36) and have shown that cell cycle arrest occurs following influenza virus infection (37). For example, similar to the aforementioned findings, airway inflammation was worsened and the cell cycle was arrested after influenza virus infection in these previous studies. Inhibiting the expression of RKIP also aggravated the inflammatory response. The present study further strengthened the hypothesis that RKIP was indeed protective against the production of cytokines and recovered cell cycle progression. Such data may greatly enhance the search for drugs that can potentially ameliorate IAV-induced inflammatory diseases.

The present results additionally revealed that airway inflammation was significantly suppressed and that cell cycle arrest was reversed with RKIP-OE *in vitro*. Congruent with our previous study, a mouse model of airway inflammation induced by IAV was successfully constructed (29,38), and revealed that inhibition of RKIP enhanced the production of cytokines and the expression of CDK4, which is closely to cell cycle progression, thus suggesting that downregulation of RKIP arrested the cell cycle after IAV infection *in vivo*. These results were similar to the *in vitro* outcomes of the present study.

It has previously been reported that reducing RKIP expression may alleviate liver fibrosis (39), and that inhibition of RKIP could lead to an improvement in hepatic fibrosis (40). These previous studies suggested that RKIP may have different roles in different organs. Although the role of RKIP is controversial with respect to different organs and organ systems, the present study confirmed that RKIP serves a protective role in airway inflammation and cell cycle progression following IAV infection.

Emerging evidence has suggested that the ERK/MAPK pathway is critically involved in numerous pathophysiological processes, including cell proliferation, stress, inflammatory responses, differentiation and apoptosis (18,41,42). However, whether RKIP mediates the IAV-induced airway inflammatory response via the ERK/MAPK signal transduction pathway remains unclear. The present study demonstrated that this pathway was activated following IAV infection; notably, in DHBE cells, RKIP inhibition did not further increase the production of IL-1β and IL-18 and cell cycle arrest when the ERK/MAPK pathway was inhibited by SCH772984 after IAV infection. These findings indicated that RKIP could protect airway epithelial cells against an inflammatory response induced by IAV via the ERK/MAPK pathway, and suggested that ERK/MAPK may be a potential pathway that mediates the anti-viral effect of RKIP. In addition, it has been consistently reported that RKIP functions as an anti-viral agent in innate immunity (43). These findings collectively reveal that RKIP constitutes a promising target for anti-viral treatment modalities, with IAV the principal pathogen in emerging respiratory infectious diseases that lack an effective therapy. The present results might therefore be of relevance in the future development of targeted treatment approaches in IAV-induced inflammatory diseases.

It has previously been demonstrated that airway inflammation is exacerbated and the cell cycle blocked after influenza virus infection (37,44), and a previous study reported that cell cycle arrest promoted viral replication to increase inflammation (44). The present study elucidated the role of RKIP in promoting recovery of the cell cycle after its arrest to alleviate the inflammatory responses induced by IAV in airway epithelial cells. Collectively, these findings suggested that the cell cycle is tightly linked to inflammatory diseases. Moreover, it has been indicated that inflammation is a critical component of tumor progression (45), and it is well known that the cell cycle is accelerated in tumor progression. Therefore, it was hypothesized that the cell cycle changes dynamically during the progression of inflammation-related diseases. With the development of inflammatory-related diseases, inflammation could progress from acute to chronic, and chronic inflammation could lead to cancer. During this progression, the cell cycle may be initially arrested followed by its acceleration. It may be hypothesized that this approach could constitute a mechanism underlying inflammation in cancer transformation.

The present study investigated the airway inflammatory response induced by IAV. It is well known that IAV infection can induce several inflammatory cytokines, including IL-1β (46), IL-18 (47), TNF-α (48), IL-6 (49), IL-8 (50) and IL-10 (51). The present study mainly measured the levels of inflammation by IL-1β and IL-18; however, the other inflammatory cytokines were not assessed. In future studies, we aim to further explore the pathways related to other inflammatory cytokines and the potential molecular mechanism of IAV-induced AECOPD.

In conclusion, the present study demonstrated that the expression of RKIP was significantly diminished following IAV infection, and that RKIP served a protective role in the alleviation of airway inflammation and in the recovery of the cell cycle after IAV infection through the activities of the ERK/MAPK pathway (Fig. 6). These actions may constitute a novel treatment option for respiratory diseases that involve IAV infection.

Acknowledgements

Not applicable.

Funding

This work was supported by the National Natural Science Foundation of China (grant no. 82070047), the Subject Construction Project of Anhui Medical University (grant

no. 2021lcxk001) and the Basic and Clinical Collaborative Research Promotion Program of Anhui Medical University (grant no. 2020xkjT061).

Availability of data and materials

The datasets used and/or analyzed during the current study are available from the corresponding author on reasonable request.

Authors' contributions

GHF and YW designed the study and revised the paper. JJY and SLW conducted the experiments, wrote the paper and analyzed the data. YYW, DWZ and LS assisted with the experiments. HMW, JLS and LY assisted with the data analysis and critically reviewed the manuscript. GHF and JJY confirmed the authenticity of all the raw data. All authors read and approved the final manuscript.

Ethics approval and consent to participate

All studies involving animals were approved by the Animal Ethics Committee of Anhui Medical University (approval no. LLSC20200117) in accordance with ethical principles. All of the participants provided written informed consent and this study was approved by the Biomedical Ethics Committee of Anhui Medical University (approval no. 20200070).

Patient consent for publication

Not applicable.

Competing interests

The authors declare that they have no competing interests.

References

1. Ellul MA, Benjamin L, Singh B, Lant S, Michael BD, Easton A, Kneen R, Defres S, Sejvar J and Solomon T: Neurological associations of COVID-19. Lancet Neurol 19: 767-783, 2020.
2. Yu X, Cai T, Fan L, Liang Z, Du Q, Wang Q, Yang Z, Vlahos R, Wu L and Lin L: The traditional herbal formulation, Jianpiyifei II, reduces pulmonary inflammation induced by influenza A virus and cigarette smoke in mice. Clin Sci (Lond) 135: 1733-1750, 2021.
3. Prigge AD, Ma R, Coates BM, Singer BD and Ridge KM: Age-dependent differences in T-Cell responses to influenza A virus. Am J Respir Cell Mol Biol 63: 415-423, 2020.
4. Choi HJ, Lim CH, Song JH, Baek SH and Kwon DH: Antiviral activity of raoulic acid from Raoulia australis against Picornaviruses. Phytomedicine 16: 35-39, 2009.
5. Callon D, Berri F, Lebreil AL, Fornes P and Andreoletti L: Coinfection of parvovirus B19 with influenza A/H1N1 causes fulminant myocarditis and pneumonia. An autopsy case report. Pathogens 10: 958, 2021.
6. Sasaki M, Ikeda H, Sato Y and Nakanuma Y: Proinflammatory cytokine-induced cellular senescence of biliary epithelial cells is mediated via oxidative stress and activation of ATM pathway: A culture study. Free Radic Res 42: 625-632, 2008.
7. Zhang C, Hein TW, Wang W, Ren Y, Shipley RD and Kuo L: Activation of JNK and xanthine oxidase by TNF-alpha impairs nitric oxide-mediated dilation of coronary arterioles. J Mol Cell Cardiol 40: 247-257, 2006.
8. Darzynkiewicz Z, Williamson B, Carswell EA and Old LJ: Cell cycle-specific effects of tumor necrosis factor. Cancer Res 44: 83-90, 1984.
9. Al-Mulla F, Bitar MS, Taqi Z and Yeung KC: RKIP: Much more than Raf kinase inhibitory protein. J Cell Physiol 228: 1688-1702, 2013.
10. Iuliano AD, Roguski KM, Chang HH, Muscatello DJ, Palekar R, Tempia S, Cohen C, Gran JM, Schanzer D, Cowling BJ, *et al*: Estimates of global seasonal influenza-associated respiratory mortality: A modelling study. Lancet 391: 1285-1300, 2018.
11. Yeung K, Janosch P, McFerran B, Rose DW, Mischak H, Sedivy JM and Kolch W: Mechanism of suppression of the Raf/MEK/extracellular signal-regulated kinase pathway by the raf kinase inhibitor protein. Mol Cell Biol 20: 3079-3085, 2000.
12. Zeng L, Imamoto A and Rosner MR: Raf kinase inhibitory protein (RKIP): A physiological regulator and future therapeutic target. Expert Opin Ther Targets 12: 1275-1287, 2008.
13. Vandamme D, Herrero A, Al-Mulla F and Kolch W: Regulation of the MAPK pathway by raf kinase inhibitory protein. Crit Rev Oncog 19: 405-415, 2014.
14. Yesilkanal AE and Rosner MR: Raf kinase inhibitory protein (RKIP) as a metastasis suppressor: Regulation of signaling networks in cancer. Crit Rev Oncog 19: 447-454, 2014.
15. Klysik J, Theroux SJ, Sedivy JM, Moffit JS and Boekelheide K: Signaling crossroads: the function of Raf kinase inhibitory protein in cancer, the central nervous system and reproduction. Cell Signal 20: 1-9, 2008.
16. Noh HS, Hah YS, Zada S, Ha JH, Sim G, Hwang JS, Lai TH, Nguyen HQ, Park JY, Kim HJ, *et al*: PEBP1, a RAF kinase inhibitory protein, negatively regulates starvation-induced autophagy by direct interaction with LC3. Autophagy 12: 2183-2196, 2016.
17. Wenzel SE, Tyurina YY, Zhao J, St Croix CM, Dar HH, Mao G, Tyurin VA, Anthonymuthu TS, Kapralov AA, Amoscato AA, *et al*: PEBP1 wardens ferroptosis by enabling lipoxygenase generation of lipid death signals. Cell 171: 628-641 e26, 2017.
18. Kaminska B: MAPK signalling pathways as molecular targets for anti-inflammatory therapy-from molecular mechanisms to therapeutic benefits. Biochim Biophys Acta 1754: 253-262, 2005.
19. Liu T, Zhang L, Joo D and Sun SC: NF-κB signaling in inflammation. Signal Transduct Target Ther 2: 17023, 2017.
20. Huang Q, Bai F, Nie J, Lu S, Lu C, Zhu X, Zhuo L and Lin X: Didymin ameliorates hepatic injury through inhibition of MAPK and NF-κB pathways by up-regulating RKIP expression. Int Immunopharmacol 42: 130-138, 2017.
21. Qin Q, Liu H, Shou J, Jiang Y, Yu H and Wang X: The inhibitor effect of RKIP on inflammasome activation and inflammasome-dependent diseases. Cell Mol Immunol 18: 992-1004, 2021.
22. Mansoori B, Mohammadi A, Ditzel HJ, Duijf PHG, Khaze V, Gjerstorff MF and Baradaran B: HMGA2 as a critical regulator in cancer development. Genes (Basel) 12: 269, 2021.
23. Zhang L, Fu Z, Binkley C, Giordano T, Burant CF, Logsdon CD and Simeone DM: Raf kinase inhibitory protein inhibits beta-cell proliferation. Surgery 136: 708-715, 2004.
24. Ma J, Li F, Liu L, Cui D, Wu X, Jiang X and Jiang H: Raf kinase inhibitor protein inhibits cell proliferation but promotes cell migration in rat hepatic stellate cells. Liver Int 29: 567-574, 2009.
25. Pnueli L, Gutfinger T, Hareven D, Ben-Naim O, Ron N, Adir N and Lifschitz E: Tomato SP-interacting proteins define a conserved signaling system that regulates shoot architecture and flowering. Plant Cell 13: 2687-2702, 2001.
26. Akaishi J, Onda M, Asaka S, Okamoto J, Miyamoto S, Nagahama M, Ito K, Kwanami O and Shimizu K: Growth-suppressive function of phosphatidylethanolamine-binding protein in anaplastic thyroid cancer. Anticancer Res 26: 4437-4442, 2006.
27. Fulcher ML, Gabriel S, Burns KA, Yankaskas JR and Randell SH: Well-differentiated human airway epithelial cell cultures. Methods Mol Med 107: 183-206, 2005.
28. Yamaya M, Nishimura H, Hatachi Y, Yoshida M, Fujiwara H, Asada M, Nakayama K, Yasuda H, Deng X, Sasaki T, *et al*: Procaterol inhibits rhinovirus infection in primary cultures of human tracheal epithelial cells. Eur J Pharmacol 650: 431-444, 2011.
29. Guo Y, Tu YH, Wu X, Ji S, Shen JL, Wu HM and Fei GH: ResolvinD1 protects the airway barrier against injury induced by influenza A virus through the Nrf2 pathway. Front Cell Infect Microbiol 10: 616475, 2020.
30. Wei YY, Zhang DW, Ye JJ, Lan QX, Ji S, Sun L, Li F and Fei GH: Interleukin-6 neutralizing antibody attenuates the hypersecretion of airway mucus via inducing the nuclear translocation of Nrf2 in chronic obstructive pulmonary disease. Biomed Pharmacother 152: 113244, 2022.

31. Livak KJ and Schmittgen TD: Analysis of relative gene expression data using real-time quantitative PCR and the 2(-Delta Delta C(T)) method. Methods 25: 402-408, 2001.
32. Kajon AE, Gigliotti AP and Harrod KS: Acute inflammatory response and remodeling of airway epithelium after subspecies B1 human adenovirus infection of the mouse lower respiratory tract. J Med Virol 71: 233-244, 2003.
33. Mc Henry KT, Ankala SV, Ghosh AK and Fenteany G: A non-antibacterial oxazolidinone derivative that inhibits epithelial cell sheet migration. Chembiochem 3: 1105-1111, 2002.
34. Zhu S, Mc Henry KT, Lane WS and Fenteany G: A chemical inhibitor reveals the role of Raf kinase inhibitor protein in cell migration. Chem Biol 12: 981-991, 2005.
35. Lin W, Ma C, Su F, Jiang Y, Lai R, Zhang T, Sun K, Fan L, Cai Z, Li Z, *et al*: Raf kinase inhibitor protein mediates intestinal epithelial cell apoptosis and promotes IBDs in humans and mice. Gut 66: 597-610, 2017.
36. al-Mulla F, Bitar MS, Taqi Z, Rath O and Kolch W: RAF kinase inhibitory protein (RKIP) modulates cell cycle kinetics and motility. Mol Biosyst 7: 928-941, 2011.
37. Zhu L, Zhao W, Lu J, Li S, Zhou K, Jiang W, Duan X, Fu L, Yu B, Cai KQ, *et al*: Influenza virus matrix protein M1 interacts with SLD5 to block host cell cycle. Cell Microbiol 21: e13038, 2019.
38. Ji S, Bai Q, Wu X, Zhang DW, Wang S, Shen JL and Fei GH: Unique synergistic antiviral effects of Shufeng Jiedu Capsule and oseltamivir in influenza A viral-induced acute exacerbation of chronic obstructive pulmonary disease. Biomed Pharmacother 121: 109652, 2020.
39. Ma J, Qiu Y, Wang M, Zhang M, Zhao X and Jiang H: Locostatin alleviates liver fibrosis induced by carbon tetrachloride in mice. Dig Dis Sci 64: 2570-2580, 2019.
40. Lin X, Bai F, Nie J, Lu S, Lu C, Zhu X, Wei J, Lu Z and Huang Q: Didymin alleviates hepatic fibrosis through inhibiting ERK and PI3K/Akt pathways via regulation of raf kinase inhibitor protein. Cell Physiol Biochem 40: 1422-1432, 2016.
41. Pearson G, Robinson F, Gibson TB, Xu BE, Karandikar M, Berman K and Cobb MH: Mitogen-activated protein (MAP) kinase pathways: Regulation and physiological functions. Endocr Rev 22: 153-183, 2001.
42. Wang X, Xing Y, Tang Z, Tang Y, Shen J and Zhang F: Thioredoxin-2 impacts the inflammatory response via suppression of NF-κB and MAPK signaling in sepsis shock. Biochem Biophys Res Commun 524: 876-882, 2020.
43. Gu M, Liu Z, Lai R, Liu S, Lin W, Ouyang C, Ye S, Huang H and Wang X: RKIP and TBK1 form a positive feedback loop to promote type I interferon production in innate immunity. EMBO J 35: 2553-2565, 2016.
44. Ho HT, Peischard S, Strutz-Seebohm N and Seebohm G: Virus-host interactions of enteroviruses and parvovirus B19 in myocarditis. Cell Physiol Biochem 55: 679-703, 2021.
45. Andrejeva G and Rathmell JC: Similarities and distinctions of cancer and immune metabolism in inflammation and tumors. Cell Metab 26: 49-70, 2017.
46. McAuley JL, Tate MD, MacKenzie-Kludas CJ, Pinar A, Zeng W, Stutz A, Latz E, Brown LE and Mansell A: Activation of the NLRP3 inflammasome by IAV virulence protein PB1-F2 contributes to severe pathophysiology and disease. PLoS Pathog 9: e1003392, 2013.
47. Ichinohe T, Pang IK, Kumamoto Y, Peaper DR, Ho JH, Murray TcS and Iwasaki A: Microbiota regulates immune defense against respiratory tract influenza A virus infection. Proc Natl Acad Sci USA 108: 5354-5359, 2011.
48. Lu H, Chelvanambi S, Poirier C, Saliba J, March KL, Clauss M and Bogatcheva NV: EMAPII monoclonal antibody ameliorates influenza A virus-induced lung injury. Mol Ther 26: 2060-2069, 2018.
49. Zhou J, Wang D, Gao R, Zhao B, Song J, Qi X, Zhang Y, Shi Y, Yang L, Zhu W, *et al*: Biological features of novel avian influenza A (H7N9) virus. Nature 499: 500-503, 2013.
50. Ito Y, Correll K, Zemans RL, Leslie CC, Murphy RC and Mason RJ: Influenza induces IL-8 and GM-CSF secretion by human alveolar epithelial cells through HGF/c-Met and TGF-α/EGFR signaling. Am J Physiol Lung Cell Mol Physiol 308: L1178-L1188, 2015.
51. Ring S, Eggers L, Behrends J, Wutkowski A, Schwudke D, Kröger A, Hierweger AM, Hölscher C, Gabriel G and Schneider BE: Blocking IL-10 receptor signaling ameliorates Mycobacterium tuberculosis infection during influenza-induced exacerbation. JCI Insight 5: e126533, 2019.